

Temperature dependences of piezoelectric properties of vanadium substituted $\text{SrBi}_2\text{Nb}_2\text{O}_9$ ceramics with grain orientation

Shinya Inai, Yuji Hiruma, Muneyasu Suzuki, Hajime Nagata, Tadashi Takenaka *

Faculty of Science and Technology, Tokyo University of Science, Yamazaki 2641, Noda, Chiba 278-8510, Japan

Available online 25 September 2007

Abstract

The temperature dependence of the piezoelectric properties of vanadium substituted strontium bismuth niobate, $\text{SrBi}_2\text{Nb}_{1.95}\text{V}_{0.05}\text{O}_9$ (SBNV) ceramics, were investigated in various vibration modes. The effects of grain orientation in SBNV ceramics on the piezoelectric properties were also studied by the hot-forging (HF) method. The anisotropy of the piezoelectric properties of each vibration mode was confirmed by observing the grain orientation. In particular, HF-SBNV ceramics of the (33) and (15) modes showed excellent piezoelectric properties with relatively high mechanical quality factors, Q_m (2200, 4600), and high electrical quality factors, Q_e max (66.0, 21.6), respectively. In addition, HF-SBNV ceramics showed low temperature coefficients of resonance frequency $TC-f_r$ (−16.5, −27.0). HF-SBNV ceramics are considered to be superior candidates for the lead-free piezoelectric application of ceramic resonators.

© 2007 Elsevier Ltd and Techna Group S.r.l. All rights reserved.

Keywords: A. Sintering; A. Grain growth; C. Piezoelectric properties

1. Introduction

Bismuth layer-structured ferroelectrics (BLSFs) have attracted much attention as candidate lead-free piezoelectric materials because of their attractive dielectric and ferroelectric properties. BLSFs have the general formula $(\text{Bi}_2\text{O}_2)^{2+}(\text{A}_{m-1}\text{B}_m\text{O}_{3m+1})^{2-}$, in which pseudoperovskite $(\text{A}_{m-1}\text{B}_m\text{O}_{3m+1})^{2-}$ layers are interleaved with $(\text{Bi}_2\text{O}_2)^{2+}$ layers, where m is the number of BO_6 octahedra in the pseudo-perovskite layers ($m = 1-5$). Fig. 1 shows the crystal structure of BLSFs ($m = 2$).

Recently, among many BLSF materials, $\text{SrBi}_2\text{Nb}_2\text{O}_9$ (SBN)-based materials have been studied as piezoelectric materials for resonator and filter applications because of their low temperature coefficients of resonance frequency $TC-f_r$ [1–3]. Our group reported that the ferroelectric and piezoelectric properties were improved by V substitution at Nb site in SBNV ceramics [4].

In addition, it is well known that the anisotropy of the crystal structure is large and the direction of spontaneous polarization is restricted to two dimensions for BLSF. Therefore, a grain orientation technique is effective in fulfilling potential of good

ferroelectric and piezoelectric properties in BLSFs, without losing the anisotropy of the single crystal as much as possible. There are several reports on the piezoelectric properties of grain-oriented BLSFs [5–7]. It has been reported that the coupling factors and piezoelectric constants are improved by grain orientation. However, there are many unknown facts about the temperature dependences of piezoelectric properties in grain orientation ceramics.

In this study, we investigated the effects of the grain orientation in vanadium substituted SBN ceramics, $\text{SrBi}_2\text{Nb}_{1.95}\text{V}_{0.05}\text{O}_9$ (SBNV), focusing on the temperature dependences of the piezoelectric properties in various vibration modes. A grain-oriented sample was prepared by the hot-forging (HF) method.

2. Experimental procedure

Ceramic samples of SBNV were prepared by a conventional sintering technique (ordinary firing, OF sample). Mixtures of SrCO_3 , Bi_2O_3 , Nb_2O_5 and V_2O_5 of purity higher than 99.9% were used as the starting materials. These mixtures were calcined at 800 °C for 2 h, then ground. The calcined powders were pressed into a cylinder 20 mm in diameter and 10 mm in thickness by uniaxial pressing followed by cold isostatic

* Corresponding author. Tel.: +81 4 7122 9539; fax: +81 4 7123 0856.

E-mail address: tadashi@ee.noda.tus.ac.jp (T. Takenaka).

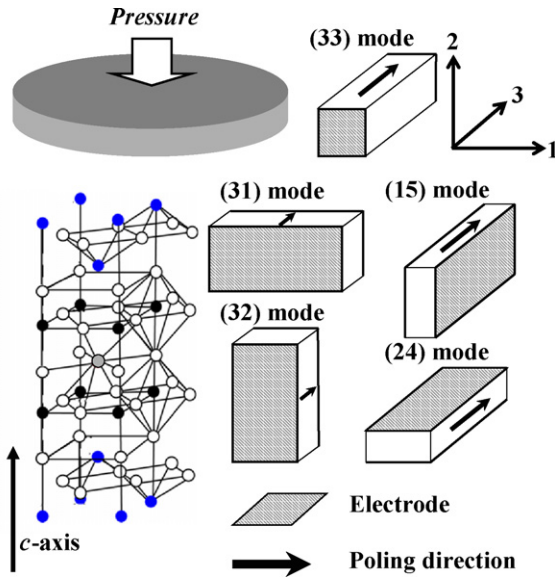


Fig. 1. Crystal structure of SBN and (33), (31), (15), (32) and (24) vibration mode specimens.

pressing (CIP) at 150 MPa. The SBNV cylinders were sintered at 950 °C for 2 h in air. Grain-oriented samples were prepared by the hot-forging (HF) method [5]. The grain-orientation factor, F , was calculated by Lotgering method [7]. The phases of the ceramic samples were identified by X-ray diffraction (XRD) analysis.

The sintered ceramics were cut and polished into appropriate shapes to determine the piezoelectric properties in various vibration modes as shown in Fig. 1. Specimens undergoing piezoelectric measurements were poled in a silicone oil bath at an applied field of 7–10 kV/mm and a temperature of 150–200 °C for 5 min. The piezoelectric properties of the poled ceramics were investigated by a resonance–antiresonance method using a precision impedance analyzer (HP 4294A). The electromechanical coupling factors, k_{ij} , were calculated on the basis of Onoe's equation using series and parallel resonance frequencies, f_s and f_p . The temperature coefficient of the resonance frequency, $TC-f_r$, was measured in the temperature range from –25 to 125 °C using a temperature controller (TABAI-ESPEC SU-240). The temperature coefficient of resonance frequency ($TC-f_r$) was calculated by the following equation:

$$TC - f_r = \frac{f_r[125^\circ\text{C}] - f_r[-25^\circ\text{C}]}{f_r[20^\circ\text{C}] \times T}$$

where, $f_r[-25^\circ\text{C}]$, $f_r[125^\circ\text{C}]$ and $f_r[20^\circ\text{C}]$ are the resonance frequencies at –25, 125 and 20 °C, respectively. T is the measurement temperature range (150 °C).

3. Results and discussion

SBNV ceramics with a relative density of more than 97% were obtained. XRD patterns for OF-SBNV ceramics show single-phase bismuth layer-structured compounds with the layer number $m = 2$. The grain orientation factors, F , of SBNV ceramics determined by the Lotgering method [7] were approximately ~100%.

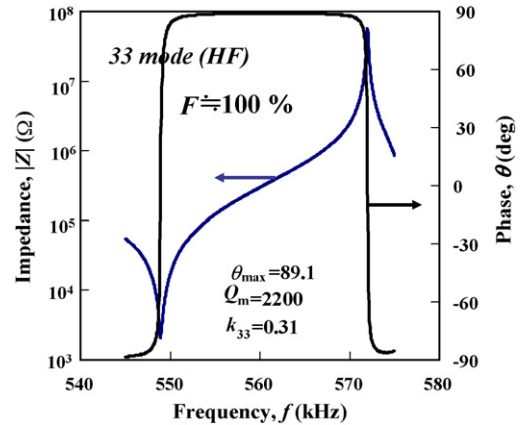


Fig. 2. Frequency characteristics of impedance, Z , of HF-SBNV ceramics.

Fig. 2 shows the frequency dependence of impedance, Z (magnitude $|Z|$, and phase θ), for the (33) mode of HF-SBNV ceramics. Fine profiles were obtained. Comparatively fine profiles were confirmed in other modes. Table 1 summarizes the piezoelectric properties of each vibration mode for OF- and HF-SBNV ceramics. The electromechanical coupling coefficients k_{33} and k_{15} of HF-SBNV are about 1.5–2 times larger than those of OF-SBNV. The electrical quality factor, $Q_{e \max}$ ($=\tan \theta_{\max}$), of the HF sample is improved in the (33) and (15) modes. The Q_m of the HF samples are lower than those of the OF samples in the (33) and (15) modes, but are still higher than 2000. These results, which agree with those of other BLSFs, are due to the grain orientation [5,6]. On the other hand, k_{24} is about the half value of k_{15} for the OF ceramics. The Q_m of the (32) and (24) modes are higher than those of the OF samples. These differences can be explained by the anisotropy of the crystal structure [8]. As a result, the anisotropy of the piezoelectric properties of each vibration mode is confirmed. In particular, HF-SBNV ceramics in the (33) and (15) modes showed excellent piezoelectric properties of $k_{33} = 31.0$, $k_{15} = 15.7$, $Q_m = 2200$ and 4600, and $Q_{e \max} = 66.0$ and 21.6, respectively.

Fig. 3 shows the temperature dependence of the resonance frequency and $TC-f_r$ value for each vibration mode. The $TC-f_r$ of the (33), (31) and (15) modes for the HF samples were –16.5, –5.0 and –27.0, respectively. These values are lower than those of OF samples. On the other hand, the $|TC-f_r|$ of the (32) and (24) modes were larger than those of the (31) and (15)

Table 1

Piezoelectric properties of each vibration mode for OF- and HF-SBNV ceramics

Mode	F (%)	k (%)	Q_m	Q_e	$TC-f_r$ (ppm/°C)	s_{**}^E
33 (OF)	–	17.5	5500	27.7	–42.1	8.44 (s_{33}^E)
33 (HF)	100	31.0	2200	66.0	–16.5	7.44 (s_{33}^E)
31 (OF)	–	4.5	7100	2.9	–46.0	8.08 (s_{11}^E)
31 (HF)	100	1.3	–	–	–5.0	7.03 (s_{11}^E)
32 (HF)	90.5	5.4	9300	5.7	–73.0	12.1 (s_{22}^E)
15 (OF)	–	10.6	5700	15.3	–67.8	21.2 (s_{55}^E)
15 (HF)	91.5	15.7	4600	21.6	–27.0	16.7 (s_{55}^E)
24 (HF)	98.1	10.0	7200	14.7	–93.8	21.6 (s_{44}^E)

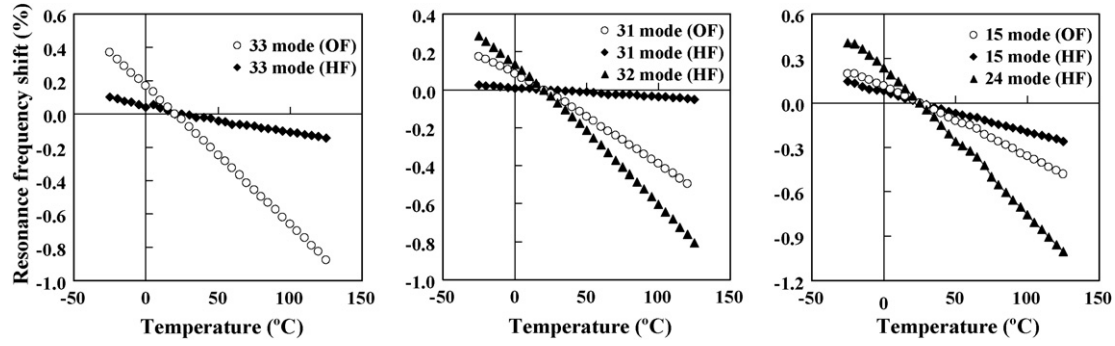


Fig. 3. Temperature dependence of the resonant frequency for each vibration mode.

modes. From these results, anisotropy of the $TC-f_r$ value in each vibration mode is clear. We are currently considering why the (33), (31) and (15) modes for the HF samples had lower $|TC-f_r|$ values.

For example, in the case of the (33) mode, antiresonance frequency, f_p , can be given by the following equation, which contains elastic compliance, s_{33}^E :

$$f_p = \frac{1}{2x} \sqrt{\frac{1}{\rho \times s_{33}^D}}, \quad s_{33}^E = \frac{s_{33}^D}{(1 - k_{33}^2)},$$

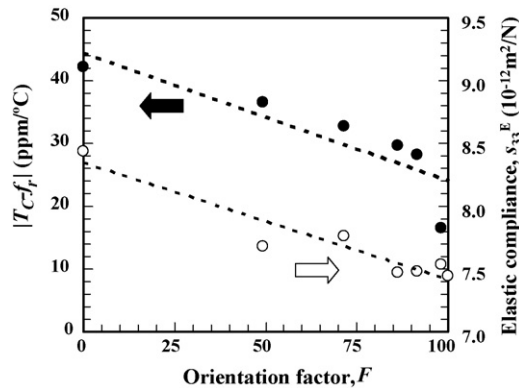
where x and ρ are the vibration length of the (33) mode specimen and the observed density, respectively. Every factor is supposed to have a temperature dependence. The thermal expansion coefficients, α , of general piezoelectric ceramics are known to be 0.5–5 ppm/°C. Here, the changes in the vibration length and density were calculated using the largest value, $\alpha = 5$ ppm/°C. Finally, the frequency change from –25 to 125 °C due to the thermal expansion of the sample was estimated, and this value was 2.47 ppm/°C. It is sufficiently small to ignore the contribution from the thermal expansion terms. However, this value is a rough estimate: thus, additional work and discussion are required. From the above speculations, the temperature dependence of elastic compliance, s_{33} , is the dominant factor in determining $TC-f_r$ values. In the case of (31), (32), (15) and (24) modes, it is considered that s_{11} , s_{22} , s_{55} and s_{44} values are related to the $TC-f_r$ value, respectively, in the same way. The elastic compliance values in each mode for

SBNV ceramics are summarized in Table 1. The s_{22}^E of the HF sample is larger than the s_{11}^E of the HF sample, which means that the vibration along the c -axis is softer than that in the a – b axes of the HF samples. The vibration along the c -axis is perpendicular to the boundary between the Bi_2O_2 layer and the perovskite block shown in Fig. 1. It is reported that the electronic hybridization between the Bi ion of the Bi_2O_2 layer and the O ion of the oxygen octahedron in the pseudo-perovskite block is low compared to other cation oxygen hybridizations in pseudo-perovskite blocks [8,9]. Therefore, the binding between the Bi_2O_2 layers and pseudo-perovskite blocks is weak. That may be one of the reasons why s_{22}^E is larger than s_{11}^E . In contrast, the s_{11}^E of the HF samples are smaller than those of the OF samples, which means that the vibration along the a -, b -axis is harder than in random directions. Fig. 4 shows s_{33}^E and $|TC-f_r|$ as a function of the orientation factor, F , in the (33) mode. The values of s_{33}^E and $|TC-f_r|$ decrease linearly with increasing orientation factor, F . The randomly oriented sample, OF, contains the a -, b - and c -direction vibrations and s_{33}^E value of the OF sample is the average of those in a , b and c directions. In other words, the s_{33}^E of the randomly oriented sample is larger than s_{33}^E in the HF sample because the randomly oriented sample includes s_{33}^E along the c direction, which has larger s_{33}^E . These results also support the above speculation about the anisotropy of the crystal structure and s_{33}^E values and suggest that anisotropy directly affects the $TC-f_r$ behavior. s_{44}^E is also larger than s_{55}^E for OF sample. The reason is that shear distortion occurs parallel to the Bi_2O_2 layers and corresponds to the motion of the Bi_2O_2 layers to the a -axis for the pseudo-perovskite blocks in the (24) mode [8,9]. In contrast, the s_{44}^E of the HF sample is smaller than that of the OF sample. These differences in elastic compliances relate to the stability of the $TC-f_r$ values. In addition, the anisotropy of the crystal structure and the Bi_2O_2 layer are related to the elastic compliances.

From these results, HF-SBNV ceramics showed excellent piezoelectric properties and $TC-f_r$ in the (33), (31) and (15) modes. Therefore, SBNV ceramics are superior candidates for lead-free piezoelectric ceramics for resonator and filter applications.

4. Conclusions

$\text{SrBi}_2\text{Nb}_{1.95}\text{V}_{0.05}\text{O}_9$ (SBNV) ceramics were studied in terms of the effects of grain orientation focusing on the temperature

Fig. 4. Elastic compliance, s_{33}^E and temperature coefficient of resonance frequency, $TC-f_r$, as a function of the orientation factor, F , in the (33) mode.

dependences of the piezoelectric properties in various vibration modes. The following results were obtained:

- (1) The anisotropy of the piezoelectric properties of each vibration mode was confirmed by observing the grain orientation.
- (2) The $|TC\text{-}f_r|$ of the grain-oriented sample in the (33), (31) and (15) modes were lower than those of nonoriented modes.
- (3) The HF-SBNV ceramics showed relatively high Q_m (2200, 4600), high $Q_{e \text{ max}}$ (66.0, 21.6) and low $TC\text{-}f_r$ (−16.5, −27.0) values in the (33) and (15) modes, respectively.

From these results, the SBNV ceramics are shown to be superior candidates for lead-free piezoelectric ceramics for resonator applications.

Acknowledgment

This work was supported in part by a Grant-in-Aid for Scientific Research (B) (No. 17360327) from the Japan Society for the Promotion of Science.

References

- [1] A. Ando, M. Kimura, Y. Sakabe, Piezoelectric resonance characteristics of $\text{SrBi}_2\text{Nb}_2\text{O}_9$ -based ceramics, *Jpn. J. Appl. Phys.* 42 (2003) 150–156.
- [2] A. Ando, M. Kimura, Y. Sakabe, Piezoelectric properties of Ba and Ca doped $\text{SrBi}_2\text{Nb}_2\text{O}_9$ based ceramic materials, *Jpn. J. Appl. Phys.* 42 (2003) 520–525.
- [3] H. Ogawa, T. Sawada, M. Kimura, K. Shiratsuyu, N. Wada, A. Ando, H. Tamura, Y. Sakabe, Piezoelectric properties of $\text{SrBi}_2\text{Nb}_2\text{O}_9$ textured ceramics, *Jpn. J. Appl. Phys.* 44 (2005) 7050–7054.
- [4] R. Aoyagi, S. Inai, Y. Hiruma, T. Takenaka, Piezoelectric properties of vanadium-substituted strontium bismuth niobate, *Jpn. J. Appl. Phys.* 44 (2005) 7055–7058.
- [5] T. Takenaka, K. Sakata, Grain orientation and electrical properties of hot-forged $\text{Bi}_4\text{Ti}_3\text{O}_{12}$ ceramics, *Jpn. J. Appl. Phys.* 19 (1980) 31–39.
- [6] T. Takenaka, H. Nagata, Grain orientation and electrical properties of some bismuth layer-structured ferroelectrics for lead-free piezoelectric applications, *Ferroelectrics* 336 (2006) 119–136.
- [7] F.K. Lotgering, *J. Inorg. Nucl. Chem.* 9 (1959) 113.
- [8] H. Ogawa, M. Kimura, A. Ando, Y. Sakabe, Temperature dependence of piezoelectric properties of grain-oriented $\text{CaBi}_4\text{Ti}_4\text{O}_{15}$ ceramics, *Jpn. J. Appl. Phys.* 40 (2001) 5715–5718.
- [9] M.G. Stachiotti, C.O. Rodriguez, N.E. Ambrosch-Draxl, Christensen, Electronic structure and ferroelectricity in $\text{SrBi}_2\text{Ta}_2\text{O}_9$, *Phys. Rev. B* 61 (2000) 14434–14439.